Biocatalysis and Agricultural Biotechnology 18 (2019) 100939

Contents lists available at ScienceDirect

Biocatalysis and Agricultural Biotechnology

journal homepage: www.elsevier.com/locate/bab

Bactericidal potential of silver-tolerant bacteria derived silver nanoparticles against multi drug resistant ESKAPE pathogens

Mohd Hashim Khan, Sneha Unnikrishnan, Karthikeyan Ramalingam*

School of Life Sciences, B.S. Abdur Rahman Crescent Institute of Science and Technology, GST Road, Vandalur, Chennai 600048, India

ARTICLE INFO

Keywords:
AgNPs
ESKAPE pathogens
Antimicrobial agents
Antibiofilm
Drug resistant
Bacillus cereus

ABSTRACT

The aim of current study is to explore the biosynthesis of silver nanoparticles (AgNPs) mediated by silver tolerant bacteria (AgTB) and its ameliorative efficacy against ESKAPE pathogens under in vitro condition. In present investigations, we have observed a metallic AgNPs from extracellular regimen via reduction of aqueous Ag + events by using $AgNO_3$ salt tolerated bacteria. This cascade was considered as potential candidates for the rapid synthesis of such AgNPs. In addition, the protective potential of AgNPs was evaluated with different procedures as MIC, MBC, and antibiofilm action against ESKAPE pathogen. In our results, AgTB identified as *Bacillus cereus* and displayed a well marked rapid synthesis of AgNPs within 3 h. The AgNPs was evaluated by using UV–vis spectroscopy and XRD. The DLS were applied to quantify the size distribution profile of AgNPs. And also, morphological were determined by using TEM study. In our result, TEM images exhibited well defined shape and size with an average particle size of about 17.51 nm. Likewise, FTIR analyses were shown marked validation with secondary metabolites which may bound to AgNPs and contributed for their stability. Our screened AgNPs showed both anti–microbial and anti–biofilm potency against multi–drug resistant ESKAPE pathogen. This bacterial mediated synthesis may be considered as an alternative approach for traditional chemical (toxic) and physical (high energy expensive) synthesis methods; and ultimately these nanoparticles can be applied for the treatment strategies for drug resistant ESKAPE pathogens.

1. Introduction

With the recent emergence of nanomaterial research, several microbiologists are now being investigating the excellent paradigm on biological synthesis of metal nano particles (MNPs). This may be put forward for their less toxicity and synthesis depending on its reduction and/or oxidation reactions in metal compounds. In this circumstance, numerous unicellular and multicellular microbes have been considered as nanofactory that are more capable to produce MNPs either by splitting or non splitting the cells followed by intracellular and extracellular methods (Bhainsa and D'Souza, 2006; Shahverdi et al., 2007a, 2007b; Jha and Prasad, 2010). Extracellular green synthesis of AgNPs mediated by natural organisms has become a major focus in the era of research due to their simplified procedure, enhanced stability, and their potential applications. These cascades can be considered as an antimicrobial agent in fatal infectious diseases, biological imaging procedures, gene silencing and targeted drug delivery (Wei and Qian, 2008). In addition to that, one more approach for appropriate rating of AgNPs as antimicrobial agents are more dominant as one of the potential alternative strategies. This may leads to combat drug resistant microorganisms including ESKAPE pathogens (*Enterococcus faecium*, *Staphylococcus aureus*, *Klebsiella pneumoniae*, *Acinetobacter baumannii*, *Pseudomonas aeruginosa* and *Enterobacter* species). Such pathogens are primarily responsible to causes hospital–acquired transmissions. In human context, lethality of pathogens is due to the development of resistance against numerous antibiotics employed to target these infectious agents (Roy et al., 2018). Recently, there are several reports published on the role of silver and its applications have been frequently disbursed with AgNPs emergence (Matthews et al., 2010; Arvizo et al., 2012; Franci et al., 2015). Based on previously advocated literatures, AgNPs exerts its multiple modes of action against diverse pathogenic microorganisms, probably due to their positive charge interaction with cell wall. This may be responsible to cause pits and ultimately leads to loss of cellular constituents, binding to thiol group of vital components and damaging the DNA which in turn suppresses the replication process of organisms (Buzea et al., 2007; Tiwari et al., 2015).

In this present study, we reported AgTB mediated synthesis and characterization of AgNPs and evaluate their efficacy on ESKAPE pathogens including *E. faecium* (MCC 2763), Methicillin–resistant *S. aureus* (ATCC 33591, MTCC 1430), *Klebsiella pneumonia* (ATCC 35657,

* Corresponding author.
E-mail addresses: hashimkhanamu@gmail.com (M.H. Khan), karthikeyan.sls@bsauniv.ac.in (K. Ramalingam).

https://doi.org/10.1016/j.bcab.2018.12.004

Available online 20 December 2018

MTCC 432), *A. baumannii*–(ATCC 19606, MTCC 1920), *P. aeruginosa* (ATCC 27853, MTCC 1688), *E. aerogenes* (MTCC 111) and *Enterobacter* species (MCC 2296) which are likely to be more responsible for induction of nosocomial infections in hospital settings and medical devices. Efficacy was tested by MIC, MBC and antibiofilm activity against multi–drug resistant ESKAPE pathogens. Furthermore, the biologically synthesized nanoparticles were characterized by UV–Vis spectrophotometer, FTIR, XRD, DLS and TEM analysis. However, the green synthesis of AgNPs using bacterial supernatant is potentially advantageous to overcome drug resistance in microorganisms by treating them through nontoxic approach, because chemically synthesized AgNP shows genotoxity, cytotoxcity and adverse immune reactions (Staszek et al., 2015; Braydich-Stolle et al., 2005).

2. Material and methods

2.1. Materials

For the identification of AgTB, Biochemical test Kit, $AgNO_3$ and all the media used in experiment were purchased from Himedia Laboratories Mumbai, India. For the preparation of all of the aqueous solutions (freshly prepared) sterile ultra pure water was used throughout the experiments. To check the efficacy of AgNPs against ESKAPE pathogens, all the strains available commercially were purchased from ATCC (American type culture collection), MTCC (Microbial type culture collection) and MCC (Microbial culture collection).

2.2. Isolation of AgTB

The surface water samples were collected from a depth of 15 cm approx from sewage–rich contaminated pond. The enrichment was performed in flasks containing silver metal for 15 days at room temperature. Sample were serially diluted and streaked on nutrient agar plates impregnated with different concentrations (100, 200, 400, 800, 1000 and 1200 μg/ml) of silver nitrate, incubated at 37 °C for 48 h. On the basis of visual observation, healthy colonies were selected and sub–cultured on nutrient agar to select pure colonies.

2.3. Phenotypic, biochemical and genotypic identification of the bacteria

Morphological and biochemical identification was done by Gram's staining and Biochemical tests performed using HilMVIC Biochemical Test Kit (Himedia). Molecular characterization of selected AgTB was carried out by 16S rRNA sequence–based method. Pure culture of the targeted bacteria was grown overnight in liquid medium (LB broth) for the isolation of genomic DNA using a method described by Sambrook and colleagues (Sambrook, 1989). The total genomic DNA was extracted from the selected isolate for the amplification by using genomic DNA isolation Kit (HiPurA DNA purification gel extraction kit–Himedia, India). PCR reaction was performed in a gradient thermal cycler (Eppendorf, Germany). Purity and quality of the isolated DNA was assured by agarose gel electrophoresis using 1.0% agarose with ethidium bromide at 60 V and conformed through Chemi–luminescent Gel–documentation Unit (BioRad, USA). The PCR product then amplified as described earlier method (Weisburg et al., 1991) by using universal primers (IDT) 16S rRNA Forward (5′–AGAGTTTGATCCTGGCTCAG–3′) and 16S rRNA Reverse (3′ GGTTACCTTGTTACGACTT–3′). The amplification of DNA was done by initial denaturation at 94 °C for 1 min, followed by 35 cycles of denaturation at 94 °C for 1 min, annealing temperature of primers was 55 °C for 1 min and extension at 72 °C for 1.5 mins. The final extension was conducted at 72 °C for 2 mins. The amplified PCR product of 16S rRNA (100 ng) was used for the sequencing with the single 16S rRNA (ITS region). Forward primer: 5′–AGAGTTTGATCCTGGCTCAG– 3′ by Sanger DNA Sequencer (Euroffin biology, Bangalore, India). Therefore, obtained sequence data of isolate was further aligned by using BioEdit program and for similarity search, BLAST analysis was used for sorting out with other related species 16S rRNA sequences obtained from GenBank. The construction of phylogenetic trees and evolutionary history was inferred using the UPGMA method (Sneath and Sokal, 1973). Finally, the Evolutionary analyses were conducted in MEGA7 for bigger Datasets (Kumar et al., 2016).

2.4. Preparation of extra cellular filtrate material

Pure healthy colony of AgTB was selected and inoculated in nutrient broth and incubated in incubator shaker at 160 rpm at 37 °C for 40 h to get dense growth. At end of incubation period, the culture was centrifuged (Eppendorf 5804R) at 8000 rpm for 15 mins at 4 °C. Filtration of the extracellular material was done to remove larger molecules from the supernatant by using Whattman No. 1 filter paper. Finally collected supernatants were used for the synthesis of AgNPs.

2.5. Extracellular biosynthesis of silver nanoparticles

For biosynthesis of AgNPs, the clear supernatant (pH 7.5) was mixed with freshly prepared 1 mM $AgNO_3$ (1:4 v/v) and the mixture was heated at constant temperature 85 °C with a magnetic stirrer for 4 h. For the optimization, the reactions between supernatant and $AgNO_3$ solution were carried out in different conditions as follows cell filtrate (2.5–7.5 ml), $AgNO_3$ (0.2–3 mM), pH (6.5–10.5) and time of incubation (0–4 h) as described previously (Ali et al., 2015). The comparative experiment for the synthesis of AgNPs was also performed by incubation of reaction mixture for 4 h at room temperature and without stirring condition. The sets of test tubes containing the same amount of extracellular material without mixing $AgNO_3$ solutions were run as a parallel control under the same temperature and stirring conditions. Gradual changes in coloration of reaction mixture turned from pale yellow to dark brown were visualized suggesting the nanoparticles synthesis episodes. After completion of its incubation period, the colored solution was centrifuged at 8000 rpm, 4 °C for 15 min followed by washing with sterile ultra pure water. The pellet was collected and then dried in a Hot air Oven (Technico Laboratory Products Pvt. Ltd.) at 80 °C for 20 h. Finally, dark brown film obtained and collected by scraping was made into powder form and stored in an air tight glass container for further confirmation by various characterization techniques UV–Vis, FTIR, DLS, TGA, XRD and TEM analyses and the biological assays.

2.6. Characterization of AgNPs by using UV–visible spectroscopy

The UV– analysis of biosynthesized AgNPs were monitored for surface plasmon resonance by the use of a double beam UV–Vis spectrophotometer (V–730 Jasco Corporation Tokyo, Japan). The reduction of Ag^+ was determined by sampling from reaction mixture periodically, the measurement of spectra operated at a resolution of 1 nm in the wavelength ranges between 350 and 800 nm. Under different experimental conditions the spectra of synthesized AgNPs were recorded time to time at intervals of 0, 1, 2, 3 and 4 h with varying conditions and parameters i.e. concentration of $AgNO_3$, ratios of supernatant and $AgNO_3$, pH, temperature and volume of reducing agent (Ali et al., 2015). During sampling time, sterile ultra pure water was used as a blank and the background absorption was subtracted. For the determination of stability of AgNPs, the measurements of spectra were covered time to time up to 4 months at regular time intervals of 24, 4 days, 4 weeks and 4 months.

2.7. X–ray diffraction measurements

Crystalline nature of the bimetallic AgNPs were studied using Scherrer's formula :$D = 0.9\lambda/\beta\cos\theta$: whereas, D is the crystal size of AgNPs, λ (1.54178 Å) is the wavelength of X–ray source used, β is the full–width–at–half maximum of the diffraction peak with XRD by coating the dried powder sample on XRD grid and spectra were

recorded by XRD system (Rigaku Corporation, Tokyo, Japan) operating at 40 kV and a current of 30 mA with Cu Ka radiation (k = 1. 5404 Å). The diffracted intensities were scanned in the region 2Θ angles from 20° to 80° (Patterson, 1939).

2.8. Dynamic light scattering (DLS)

The size distribution profile of biosynthesized silver nanoparticles was studied using DLS (Malvern Zetasizer Nano ZSP instrument). The size distribution of AgNPs is observed ranges from 45 to 140 nm. The calculated average particle size distribution of AgNPs is 78.8 nm. The diameters and PDI were analyzed in acquisition time 60 s, at 25 °C. As a reference dispersive medium, ultrapure water with a refractive index of 1.330, viscosity of 0.8872 cP, and a dielectric constant of 78.3 was used. For DLS measurement, the colloid was passed through a 0.2 μm pore sized PVDF (Polyvinylidene difluoride) membrane. The mean result was recorded, for which the sample was loaded into disposable sizing cuvette and the measurements were recorded thrice (Cascio et al., 2015).

2.9. Fourier transform infrared (FTIR) analysis

FTIR spectroscopy analysis carried out for the investigation of functional group responsible for surface capping of AgNPs synthesized from extracellular materials of bacterial supernatant. The creditworthy functional groups for biosynthesis of AgNPs analyzed by using JASCO–FTIR 6300 Type A, Serial No., A021161024. In brief, oven dried powder sample were applied to the surface of the diamond crystal then locked in a clutch chamber for the measurement of spectra at scanning speed 2 mm/sec in transmittance mode from 400 to 4000 cm^{-1} at 4 cm^{-1} resolution with 32 scans (Singh et al., 2011).

2.10. High resolution transmission electron microscopy (HRTEM) analysis

The size and morphological characteristics of biosynthesized AgNPs obtained by the use of culture supernatant of AgTB were evaluated for their composition by High resolution transmission electron microscope (JEOL JEM 2100, Japan). The dried samples were suspended in ethanol and sonication was also done for 20 min. After well dispersion, sample spotted on the carbon coated copper grid with 200 mesh and kept for drying at ambient temperature. The instrument was operated at 200 KeV with selected area electron diffraction (SAED) and d–spacing were examined in its high resolution mode (Singh et al., 2014). The filament was used LaB6. As a result, AgNPs were observed and images were recorded. For the evaluation of size distribution as in histogram, more than 100 particles were considered from multiple TEM micrographs and measured their size as an average count.

2.11. Antimicrobial activities of biosynthesized AgNPs against ESKAPE pathogens

2.11.1. Evaluation of minimum inhibitory and minimum bactericidal concentrations of AgNPs on ESKAPE pathogens

The assessment of Minimum inhibitory concentration (MIC) and minimum bactericidal concentration (MBC) of AgNPs against ESKAPE pathogens *E. faecium* (MCC 2763), Methicillin–resistant *S. aureus* (ATCC 33591, MTCC 1430), *Klebsiella pneumonia (*ATCC 35657, MTCC 432), *A. baumannii*–(ATCC 19606, MTCC 1920), *P. aeruginosa* (ATCC 27853, MTCC 1688), *E. aerogenes* (MTCC 111) and *Enterobacter* species (MCC 2296) were determined following the Micro-dilutions method, described by Balouirin et al. (2016) with bacterial inoculums of 1–5 × 10^6 CFU/ml and with AgNPs concentrations ranging from 500 to 7.81 μg/ml in triplicate. Sterile ultrapure water with media but without bacteria and media with bacteria in same volume was used as a positive and negative control respectively. The Microtitter plate containing treated with AgNPs and untreated ESKAPE pathogen strains as a control were incubated for 18 h at 37 °C in Incubator. The MIC was defined as the lowest concentration of any antimicrobial factors that depict no visible turbidity as growth (99% inhibition) of the microorganisms. After the completion of incubation period, 5 μl of suspension drops plated on Nutrient Agar in triplicate for 18 h at 37 °C for further investigation of growth to determine the bactericidal concentration. MBC value corresponding to the endpoint of the active growth of microbial population and defined as the lowest concentration of any antimicrobial factors that may kill (inhibits 99.9%) initial bacterial population.

2.11.2. Antibiofilm activity of AgNPs against ESKAPE pathogens

The biofilm formation in plastic Microtitter plates was performed as previously described by Ramalingam et al. (2011) with slight modifications. Briefly, 10% (150 μl) portion of an overnight grown bacterial suspension (10^7 CFU/ml) was added to each well except blank of a 24–well tissue culture plate and maintained a total of 1.5 ml volume with NB broth. The plates were incubated aerobically in Incubator shaker at 37 °C, with shaking condition at 100 rpm, for 72 h. After every 12 h intervals, the medium containing suspended bacterial cells was changed with an equal volume of fresh broth medium. Negative controls were obtained by incubating the Microtitter plates with media and inocula but without any antimicrobial agent. Blank controls were maintained by incubating plates with media without inocula. To determine the antibiofilm efficacy of AgNPs, three independent experiments were performed. Afterward the completion of incubation period (72 h) the supernatant media was removed and all the biofilms formed by microbes were treated with two different concentrations, 50 μg/ml and at sub–MIC concentrations of AgNPs against all ESKAPE pathogens for 30 min at room temperature in aseptic condition without agitation. As a positive control, 20% (v/v) Hydrogen peroxide (H_2O_2) was used. Following this, AgNPs and H_2O_2 was discarded and the wells were gently washed twice with sterilized ultra pure water.

The quantification of viable cells in biofilms in plastic Microtitter plate was performed. Fixing of attached bacteria in wells was done by using 1.5 ml 100% methanol for 15 mins. The plates were then evacuated and air dried in sterile condition. Dried well were then stained with 1.5 ml of 0.5% (w/v) crystal violet. The Microtitter plates were washed twice uniformly to rinse off excess stains by using washed bottle. The Microtitter plates then were air dried and the dye bounded adherent cells were removed with l.5 ml of 33% (v/v) Acetic acid glacial LR per well. The biomass of resulting solution was quantified by measuring the absorbance of the solubilized dye which was read as an optical density at 590 nm. The Optical density (OD) values obtained from the two duplicate wells as a mean of the absorbance. Final readings were expressed as an average OD and compared with the negative control values.

3. Results and discussion

3.1. Isolation of AgTB

Most silver salt tolerated (1000 μg/ml) colonies obtained from $AgNO_3$ impregnated nutrient agar plate and selected of the AgTB was used for biosynthesis of AgNPs. AgTB strain showed superior ability and potential to reduce Ag^+.

3.2. Phenotypic and biochemical identification of AgTB

Phenotypic characterization of the AgTB revealed that the bacterium was Gram positive rod-shaped, motile, beta hemolytic bacterium. The AgTB isolates were screened on the basis of their morphological characteristics and healthy pure colony was selected. The primary step in selection was to identify the genus *Bacillus* by motility nature on sloped agar plate. Purified selected microbes were stored on nutrient agar showed pale cottony colonies in plate. Several biochemical tests were done for further characterization of *Bacillus* sp. For the validation of results, HilMVIC (Himedia) kit containing 12 tests was

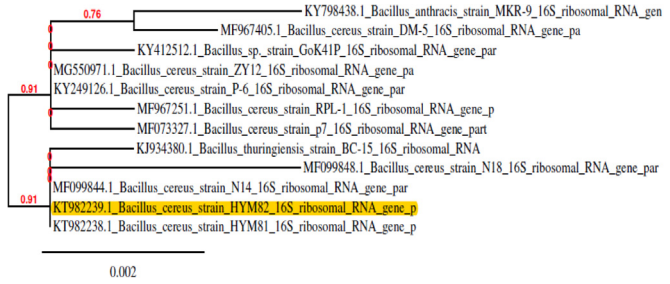

Fig. 1. The phylogenetic analysis of the 16S rRNA sequence of isolate (AgTB) obtained in the study along with other selected sequences from database. The analysis was conducted in MEGA7 for bigger Datasets. The various species of *Bacillus* available in database, phylogenetic tree showed a cluster with *Bacillus cereus*.

used to perform the biochemical identification. The results revealed that the selected AgTB isolates were *B. cereus* as showed and the characters were studied by using Bergey's manual of determinative bacteriology (Holt et al., 1994).

3.3. Genotypic characterization of AgTB

For the genotypic identification of the selected isolate was further subjected to molecular level analysis by 16S rRNA sequencing-based method to know the synthesis ability of selected one. The sequence data were subjected to NCBI BLAST analysis and the results were aligned with various *Bacillus* sp. and shared maximum similarities with *Bacillus cereus* (Fig. 1).

3.4. Extra- cellular biosynthesis of AgNPs

Ecofriendly and non toxic synthesis of AgNPs use bacterial release secondary metabolites, proteins, fats, enzymes and other biomolecules for the synthesis of silver nanoparticles and used against many drug-resistant Gram positive and negative bacteria as a weapon (Verma et al., 2018). The uses of psychrophiles, mesophilies, osmophiles and thermophiles have been reported including gram positive (*S. aureus*, *Lactobacillus* spp, *Exiguobacterium mexicanum*, *Nocardiopsis* spp, *Corynebacterium* spp, *Arthrobacter gangotriensis*) and gram negative (*Pseudomonas* spp, *Stenotrophomonas maltophilia*, *Vibrio* spp, *Idiomarina* spp, *A. baumannii*, *Alteromonas macleodii*, *Thiobacillus ferrooxidans*, *K. pneumoniae*, *Enterobacter aerogenes*, *Aeromonas* spp, *S. typhimurium* and *Escherichia coli*) for the biosynthesis of silver nanoparticles (Das et al., 2014; Iravani, 2014; Chokriwal et al., 2014; Abo-State and Partila, 2015; Kushwaha et al., 2015). In this study, rapid procedure has been exploited by using the supernatant of AgTB for the synthesis of tiny functionalized AgNPs.

The procedure of biosynthesis of silver nanoparticles is depicted in Fig. 2 at which the spectra were recorded with subsequent time to represent the approaches. The pictures and graphs are reflecting that the supernatant of AgTB and $AgNO_3$ when mixed in a set of test tubes containing total volume 15 ml in a ratio of 1:4, solutions displayed a gradual change in their appearance colour from yellowish brown to dark brown in the reaction vessels after 3 h at 70 °C (Fig. 2 A and B). The appearance of a dark brown colour in test tubes suggested the formation of AgNPs upon the completion of the 3 h reaction with $Ag+$ and supernatant (Shahverdi et al., 2007a, 2007b; Kumar et al., 2007). Gradual changes in colour considered as a preliminary indication of the formation of AgNPs in reaction mixture. The AgNPs were characterized by UV–vis spectroscopy; the technique is very useful for the primary analysis of nanoparticles. UV- spectra shows strong peaks at 422 nm is imputed to the surface plasmon resonance of AgNPs. The intensity of the functionalized AgNPs change in colour were risibly found with the time and heat when the reaction was completed and AgNPs formed due to the reduction of aqueous Ag ions. The change in colour was due to reduction of silver ion by biomolecules and enzymes present in the cell-free extracts (Fig. 2 C). The development of colour in reaction mixture is due to the excitation of surface plasmon resonance in the presence of various bio-reductant molecules (Oladipo et al., 2017). The classical representation for the synthesis of nanoparticles based on zero-order approach could be classified into three clear-cut raising phases: nucleation of the particles, progression of nuclei into seeds and the development of seeds into nanocrystals. The pattern of the formation of nanocrystals into a final shape initially determined by the internal structure of the corresponding seed and the affinity to bind the surface of the particles known as capping agents (Brust et al., 1994). Previous studies suggested that the variation in reaction carried out conditions like temperature, concentration of the $AgNO_3$, pH and storage time of the synthesized AgNPs may be affected with their shape, size, stability and production of the nonmaterial (Qu et al., 2010; Deepak et al., 2011; Heydari and Rashidipour, 2015). AgNPs synthesis was optimized with different $AgNO_3$ concentrations, temperature, pH and time (Fig. 3).

3.4.1. Influence of increasing concentrations of $AgNO_3$ on reaction

By varying the concentrations of $AgNO_3$ the assemblies of AgNPs were different due to the enzyme substrate kinetics. There is a need for the availability of the enough active site to react with the substrate molecules thus due to this phenomenon the active site within the key biomolecules that was responsible for the reduction of Ag ions become limited and the active sites was already engaged. Moreover in reaction mixture there are no more active sites left for added ions to get reduced, hence we can conclude that there is no further increase in synthesis of AgNPs despite the addition of additional nitrate salt (Singh et al., 2013). It is clear from the enzyme kinetics action that the highest optical density found up to at 1.0 mM was most by attending high intensity of reduction and produced a sharp peak at 422 nm, since beyond that the bioreduction of particles gradually decreased and peaks were become wider at the absorbance of 422 nm (Fig. 3A).

3.4.2. Influence of temperature on reaction

The rise in temperature began from room temperature to 80 °C, the peaks became sharper and sharper due to the surface plasmon resonance and at this point an absorption band at 422 nm was obtained (Fig. 3B). In standardization part, it was noticed that the synthesis of AgNPs was rapid at elevated temperature at 80 °C and the maximum formation of particles was resulted (Kannan et al., 2013) by obtaining the spectra at a specific absorbance (422 nm).

3.4.3. Effect of pH on reaction and stability of AgNPs at various time intervals

The effects of pH in reaction mixture directly attract the morphological character as well as size and shape of nanoparticles. The pH values increases the surface plasmon resonance peak shifts towards the shorter wavelengths and peak becomes sharper that show the change within the size of AgNPs. Hence raising the pH of the solution can impact the shifts of the peak near to the short wavelength and produce smaller sized nanoparticles (Alqadi et al., 2014). The stability of synthesized AgNPs was estimated for their efficacy at different time intervals and the spectra were recorded (Paredes et al., 2014). The particles were less stable in wet condition at 4 and 24 h while after 4 days, 4 weeks and 4 months it was observed that the particles stored in dried form were more stable as a function and dispersion but the peaks became wider than sharper, (Fig. 3 C) indicating the agglomeration of the particles.

3.5. XRD analysis of AgNPs

The typical XRD patterns were obtained from the sample to confirm the crystalline nature of silver nanoparticles. The X-ray diffractograms of AgNPs synthesized by the bacterial supernatant showed four intense

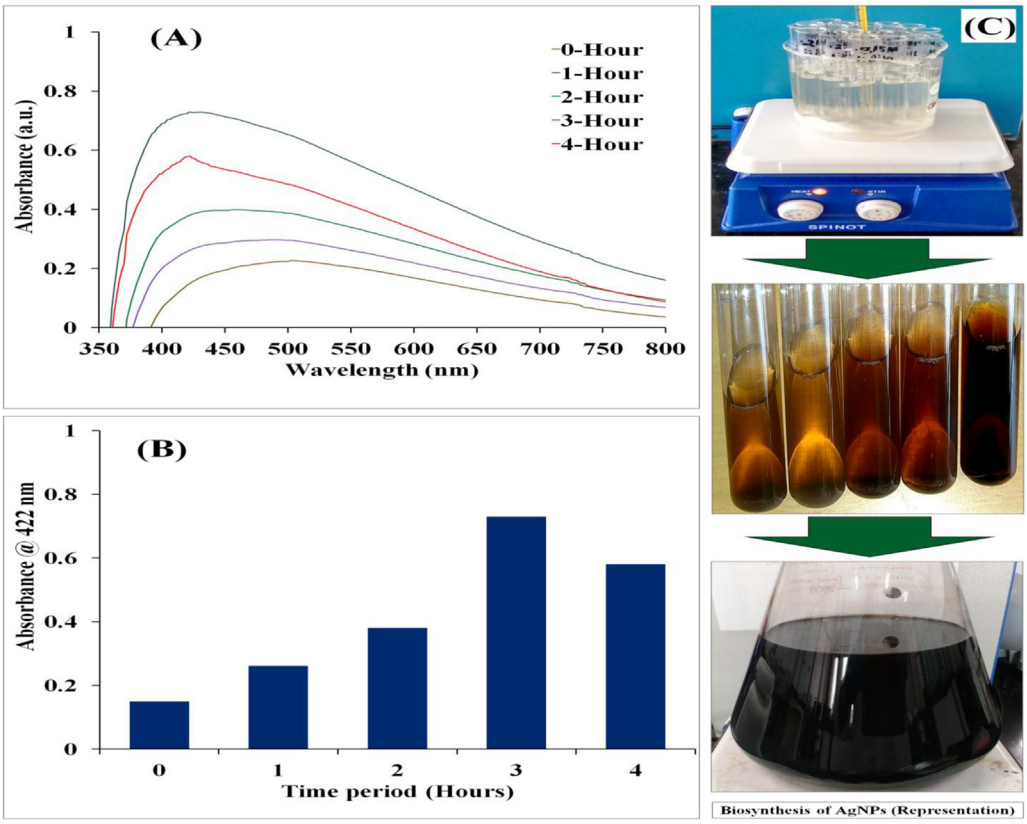

Fig. 2. UV–Vis spectrum of AgNPs synthesized by supernatant of AgTB: Panels show absorbance measurement during AgNPs synthesis as a function of different time intervals with colour change observation, (**A**) Spectra represents stirring time as 0, 1, 2, 3 and 4 h at constant temperature 70 °C; (**B**) UV–vis absorption spectra of AgNPs at a particular absorbance (422 nm) as a function of time; (**C**) Classical representation for the synthesis of AgNPs showing the pattern of colour change and bulk synthesis.

and five mild peaks in the diffraction range of 2θ values from 10° to 80° (Fig. 4A); agree with the Braggs's reflections of silver nanocrystals which are reported by Ojha et al. (2017). The peaks at 2θ values 27.84, 32.24, 38.19, 44.06, 46.25, 54.82, 57.48, 64.48, 77.39 corresponding to the [210, 122, 111, 200, 231, 142, 241, 220, 311] planes of the face centered cubic silver, respectively (JCPDS, file No. 04–0783) which suggested the crystalline nature of biosynthesized silver nanoparticles and are the similar results already reported by Meng (2015). However, the presence of some other peaks may correspond to proteins/bio-organic phase on the surface of silver nanoparticles (Vanaja and Annadurai, 2013).

3.6. FTIR analysis

This technique was done to determine the role of biomolecules and the involvement of functional groups in relation with metal salt. The FTIR analysis used to investigate the action of biomolecules and responsible factor for capping and stabilization of nanoparticles (Medina et al., 2009). The intermolecular forces (hydrophobic and hydrophilic interactions) are another factor which may involve in prevention of nanoparticles to aggregate. Powdered form of dried AgNPs obtained by the interaction of AgTB supernatant and aqueous $AgNO_3$ was used for FTIR analysis. The measurement of spectrum was carried out to spot the possible interactions between silver and bioactive molecules and capping agents available in the bacterial supernatant could be responsible for the synthesis and stabilization of AgNPs (Fig. 4B). The IR spectrum of applied sample showed band intensities in different regions at 553.47, 1069.33, 1629.55, 2110.71, 2919.69, 3302.49 corresponds to alkyl halides (C-Br)- playing an important role in bioactivity, aliphatic amines (C-N)- donating properties to stabilising molecules, 1° amines (N-H)- responsible for increase polarity, reactivity and labelling of peptides/proteins (Patil et al., 2013), alkynes (C≡C)- attributes in tagging of biomolecules including nucleic acids, proteins, lipids and glycans (Hong et al., 2014), nitriles (C≡N)- showing excellent vibrational probes of proteins for making up structural format of the particles (Lindquist et al., 2009), alkanes (C-H)- most of the alkanes are enzyme-mediated and synthesized by bacteria, responsible for saturation and unsaturation of molecules present in medium (Winter and Moore, 2009), carboxylic acid (O-H)- play a key role in active reduction of metal ions and oxidation of biomolecules, followed by nanoparticle formation (Makarov et al., 2014) respectively. Based on these amazing roles of functional groups and earlier reports, the results of present study concluded that the proteins present in the bacterial supernatant capped and stabilized the AgNPs (Kopp et al., 2017). The stabilization of nanoparticles depends on the protein-nanoparticles interactions (Vogt et al., 2015). These fundamental interactions occurred either through cysteine residues present in protein or free amino groups controlled by electrostatic forces of negatively charged carboxylic groups in enzymes (El-Deeb et al., 2013).

3.7. DLS analysis

The dynamic light scattering (DLS) pattern of the dried AgNPs dispersed in liquids medium (ultra pure water) depicted in Fig. 4C which were synthesized by using bacterial supernatant. The size distribution histogram of DLS predicted that the average diameter size of the synthesized nanoparticles is 78.8 nm and PDI value 0.491. It was noticed that the size measured through DLS is slightly larger than the size evaluated by TEM. These differences reflect the fact that TEM only measures a number based size distribution of the physical size and does not include any bio capped agent. DLS size evaluation is based on the whole hydrodynamic diameter of particle including surface capping of particles, ions or molecules that are attached to the surface which are able to travel with the AgNPs in aqueous solution (Erjaee et al., 2017). So, the hydrodynamic diameter of nanoparticles is always greater than the size estimated through the TEM analysis. Single peak found in analysis, indicated the quality of the synthesized silver nanoparticles. High intensity distribution at lower range of particle size indicates that

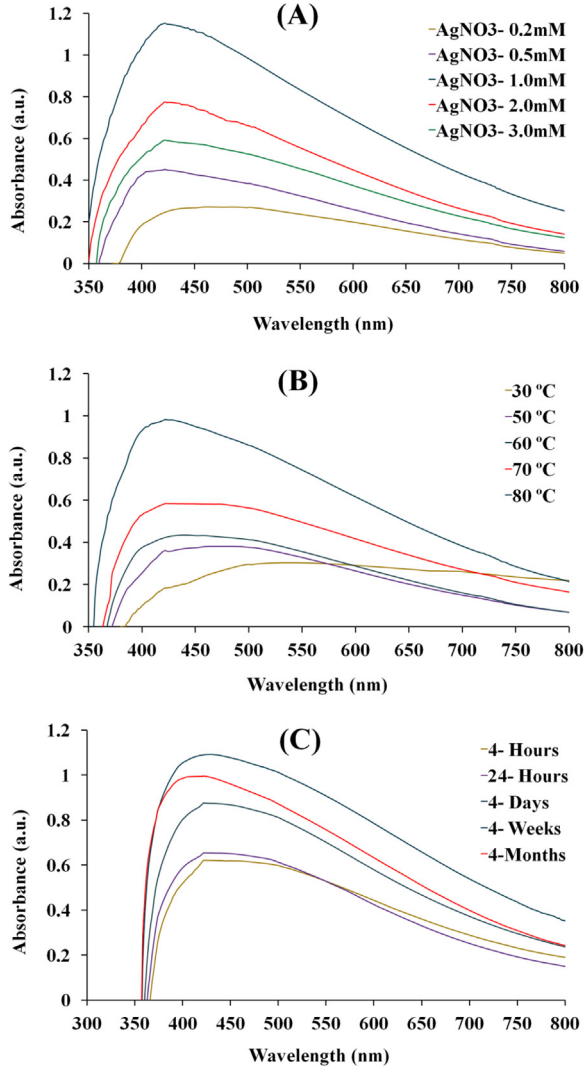

Fig. 3. UV–vis absorption spectra of AgNPs: Spectra recorded under different reaction conditions during synthesis, **(A)** $AgNO_3$ concentrations (0.2, 0.5, 1, 2 and 3 mM in presence of 3 ml AgTB supernatant with $AgNO_3$ in 1:4 v/v); **(B)** Temperature °C (30, 50, 60, 70 and 80 ^{0}C in presence of 1:4 v/v supernatant and $AgNO_3$); **(C)** Stability of the biosynthesized AgNPs as a storage time period (4 h, 24hrs, 4 days, 4 weeks and 4 months).

the most of the synthesized particles are in lower range of particle size.

3.8. Ultra high resolution transmission electron microscopy (UHRTEM) analysis

To determine the clear shape, size and morphology of biosynthesized AgNPs, they were scanned at high resolutions by using UHRTEM. In present study, the microgram of UHRTEM exhibit pleomorphic morphology including rectangular as well as hexagonal shape but the majority of particles are in spherical shape with a smooth surface (Fig. 5A, B, C and D). The dried powder of AgNPs were well dispersed into ultra pure water and evenly spread on the entire surface of the copper grid coated by carbon supported film. After drying the grid containing sample was imaged at different resolutions. Selected area electron diffraction (SAED) pattern showed predominantly presence of silver elements with its crystalline property by forming homocentric ring with bright spots of diffraction distributed on ring like circles. The pattern of diffraction rings could be indexed on the basis of the face-centered cubic (fcc) structure of silver. The development of rings due to Bragg's reflection moving back from separate rings crystal which forms spot corresponding to the presence of (111), (200) and (220) lattice planes of fcc silver nanoparticles. The same pattern was observed in XRD spectrum which conform crystallinity of AgNPs (Singh et al., 2016). The histogram of particle size represent that the majority of nanoparticles were at maximum count (38.5%) with an average size 17.5 ± 0.08 nm and all other particles showed an average size ranges from 12.5 to 47.5 nm. The size evaluated by TEM analysis and compared with DLS technique analyzer were somewhat lower. The variation in size and shape may be due to the dispersion and various biological reductants used in synthesis process (Kulkarni et al., 2015). In TEM images, biological component cap were observed which can be identified as black spot on the surface of particles.

3.9. Antimicrobial activities of biosynthesized AgNPs against ESKAPE pathogens

3.9.1. Minimum inhibitory concentration (MIC) and minimum bactericidal concentration (MBC) against ESKAPE pathogens

The antimicrobial properties of synthesized silver nanoparticles were determined by means of MIC and MBC. MIC was recorded as the lowest concentration at which no visible growth of the test pathogens was observed. MIC values of the AgNPs against ESKAPE pathogens presented in Fig. 6. The micro-dilution method was performed to determine the bacteriostatic activity and drop plate method to determine bactericidal activity of AgNPs. Biosynthesized AgNPs showed bacteriostatic and bactericidal efficacy in the range of 07.81–62.50 µg/ml and 15.62–250 µg/ml respectively, against all test pathogens. The antimicrobial proficiency of the AgNPs exhibited as MIC and MBC values against *E. faecium* (MCC 2763), *S. aureus* (ATCC 33591 (MRSA), MTCC 1430), *K. pneumoniae* (ATCC 35657, MTCC 432), *A. baumannii-* (ATCC 19606, MTCC 1920), *P. aeruginosa* (ATCC 27853, MTCC 1688) *E. aerogenes* – (MTCC 111) and *Enterobacter* sp. (MCC 2296) were estimated and depicted in Table. 2. In present study it was observed *P. aeruginosa* (ATCC 27853) blood isolate showed more susceptibility compared with *K. pneumoniae* (MTCC 432) and MRSA (ATCC 33591) against AgNPs. Therefore, our present investigations are focusing with confirmed evidences with the exposures of synthesized AgNPs are more potent or act as an inhibitor for the replication of all the used strains of ESKAPE pathogens. The efficacy of AgNPs may vary strain to strain followed by concentrations of nanoparticles. This variation may be due to cell wall structure of Gram positive bacteria- a thick makeup of peptidoglycan to enter inside the bacterial cell. In case of Gram negative the presence of lipopolysaccharide-lipoprotein complexes in the bacterial cell wall may prevent to enter the AgNPs through the wall and to reach the sensitive intracellular targets (Rudramurthy et al., 2016). Some other factors including, a rigid layer of peptidoglycan present in both the bacteria, modification of the metabolic pathways, decreased permeability which is dependent on size of the nanoparticles and increased active flux which may leads to minimize intracellular accumulation of antimicrobial agents (Schmieder and Edwards, 2012). Nevertheless, the bacteriostatic and bactericidal effects of synthesized AgNPs have been strongly confirmed to have antimicrobial potential against ESKAPE pathogens.

3.9.2. Antibiofilm activity of AgNPs against ESKAPE pathogens

The formation of biofilms is complex bacterial populations and the strategy for the estimation of microbial sustainability as well as the progression of the disease that resist the action of antibiotics. Due to the secretion of different surface molecules and virulence factors, associations of antibiotic resistant gene in bacteria promote to form a matrix. The matrix of biofilm is primarily made up of EPS consisting of polysaccharides, proteinaceous substances, glycopeptides, lipids and lipopolysaccharides which may be provided both the internal and external strength to the support and to hold together (Flemming and Wingender, 2010). In this scenario, biologically synthesized AgNPs were tested for the estimation of antibiofilm activity mediated by ESKAPE pathogens.

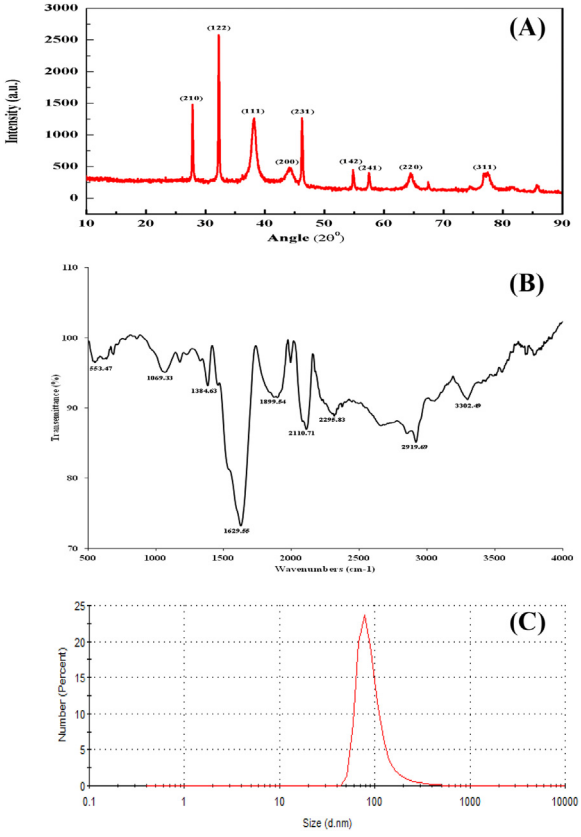

Fig. 4. Characterization of AgTB derived AgNPs: X-ray patterns (A), FTIR spectra (B), and Dynamic light scattering (C).

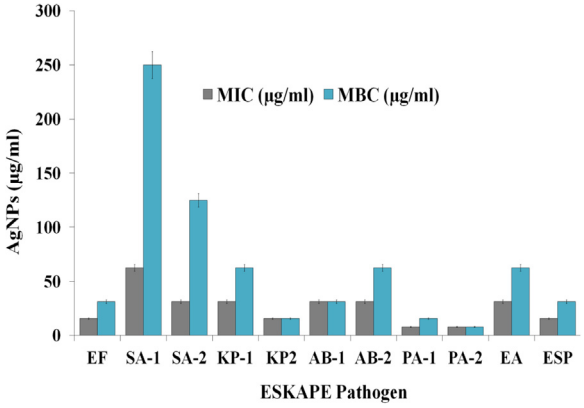

Fig. 6. Minimum inhibitory concentration (MIC) and minimum bactericidal concentration (MBC) of AgTB mediated AgNPs (EF = *E. faecium* (MCC 2763), S-1 = MRSA (ATCC 33591), S-2 = *S. aureus* (MTCC 1430), KP-1 = *K. pneumoniae* (ATCC 35657), KP-2 = *K. pneumoniae* (MTCC 432), AB-1 = *A. baumannii* (ATCC 19606), AB-2 = *A. baumannii* (MTCC 1920), PA-1 = *P. aeruginosa* (ATCC 27853), PA-2 = *P. aeruginosa* (MTCC 1688), EA = *E. aerogenes* (MTCC 111), and ESP = *Enterobacter* sp. (MCC 2296).

Similar studies revealed that AgNPs are the potential candidate which exhibited antibiofilm activity against human pathogens (Markowska et al., 2013). The biofilm formed after 72 h through each strain was evaluated for 30 mins and further treated with 50 µg/ml and sub-MIC concentration of AgNPs. The observed results of antibiofilm activity of AgNPs at all the tested sub-MIC concentrations exhibited significant biofilm reduction compared with control values (Fig. 7 A). Further evaluation of the equivalent dose of AgNPs (50 µg/ml) to all ESKAPE pathogens revealed the increasing concentration dependent breakage of biofilm when compared with positive (H_2O_2) and negative (untreated)

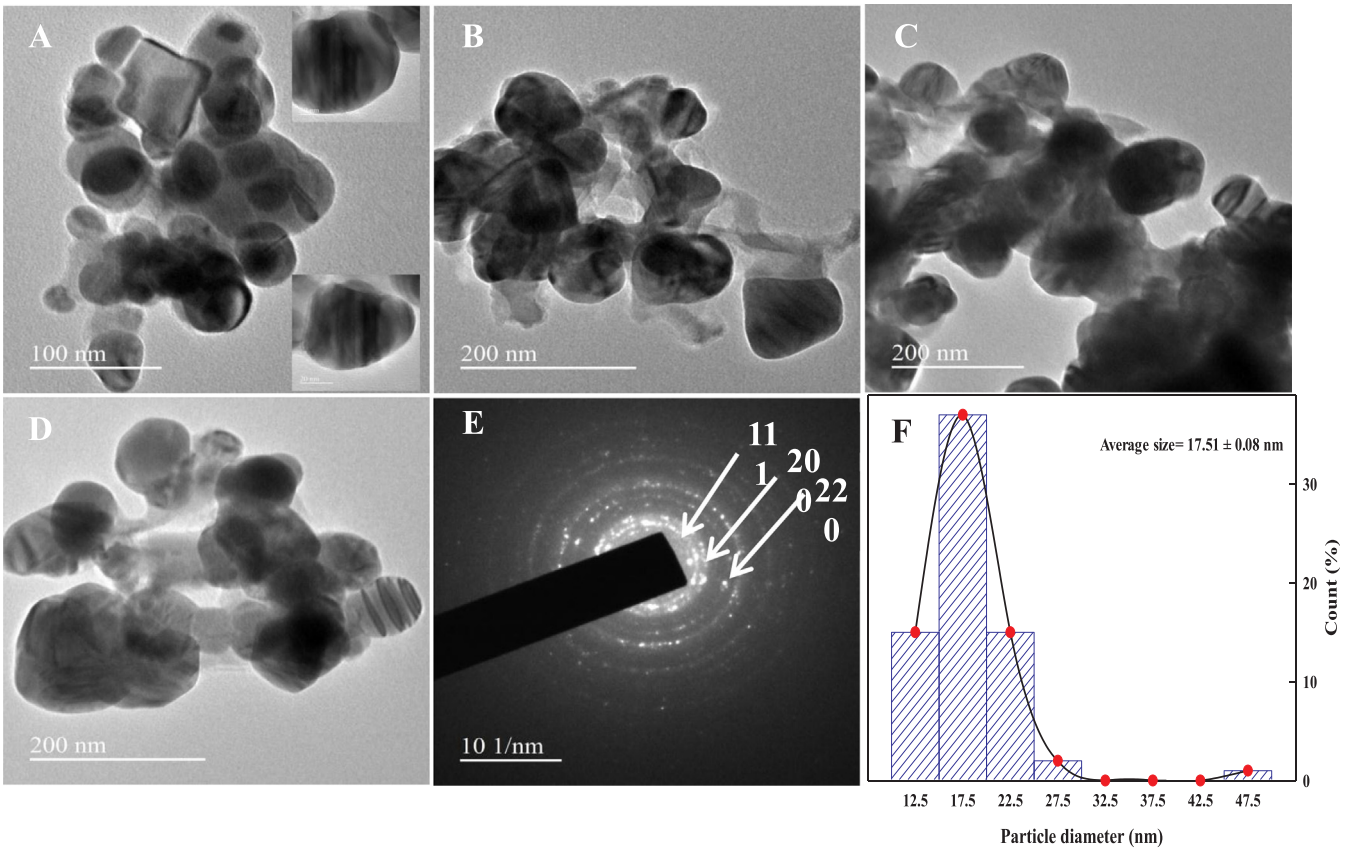

Fig. 5. HR-TEM images **(A-D)**, SEAD pattern **(E)**, and **(F)** size distribution of AgTB mediated synthesis of AgNPs.

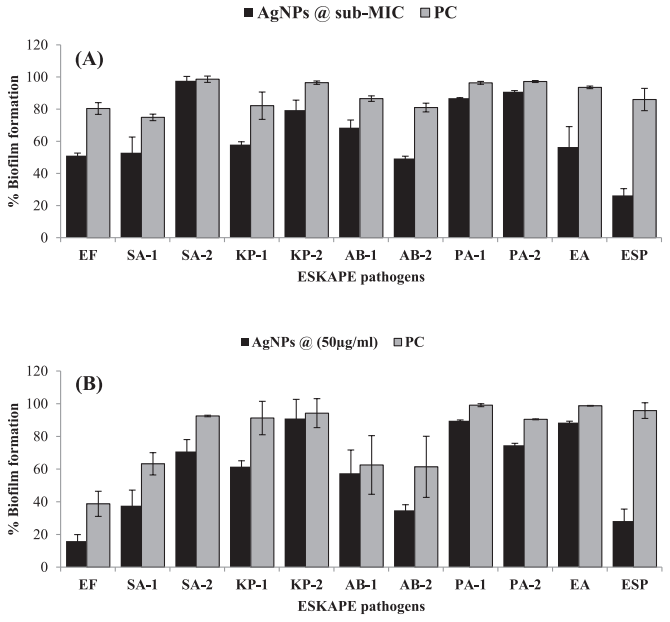

Fig. 7. Antibiofilm effect of AgTB derived AgNPs on growth of biofilms formed by ESKAPE pathogens: (A) Inhibition activity at sub-MIC concentrations of AgNPs (µg/ml), **(B)** at 50 µg/ml AgNPs. (EF = *E. faecium* (MCC 2763), S-1 = MRSA (ATCC 33591), S-2 = *S. aureus* (MTCC 1430), KP-1 = *K. pneumoniae* (ATCC 35657), KP-2 = *K. pneumoniae* (MTCC 432), AB-1 = *A. baumannii* (ATCC 19606), AB-2 = *A. baumannii* (MTCC 1920), PA-1 = *P. aeruginosa* (ATCC 27853), PA-2 = *P. aeruginosa* (MTCC 1688), EA = *E. aerogenes* (MTCC 111), and ESP = *Enterobacter* sp. (MCC 2296).

control (Fig. 7 B). Among all tested pathogens *E. faecium* (MCC 2763), MRSA (ATCC 33591), *A. baumannii*- (ATCC 19606), *A. baumannii* (MTCC 1920) and *Enterobacter* sp- (MCC 2296) the biologically synthesized AgNPs indicating the better efficacy of the nanoparticles in disrupting existing biofilms and can conclusively be delivered as an effective antibiofilm agent in further bacterial studies.

4. Conclusion

The present study based on the extracellular biogenic synthesis of AgNPs form AgTB (*Bacillus cereus*) isolated from the contaminated pond water. Here, we reported a facile, simple, efficient, and rapid method for the synthesis of AgNPs using filtered supernatant. The reaction parameters were optimized by varying time, temperature, pH, concentration and stability which resulted in maximum reduction and size effective activities, predominantly spherical in shape ranges 12.5–47.5 nm. The resulted nanoparticles were characterized by UV–Vis spectroscopy; FTIR analysis showed capping of the nanoparticles responsible for stabilization of synthesized particles; XRD and SAED analysis conformed that the particles were crystalline and metallic nature; UHRTEM analysis conformed the morphological characters of nanoparticles like shape and size distribution. The biologically functionalized silver nanoparticles exhibited excellent broad-spectrum antimicrobial activity against ESKAPE pathogens including multidrug resistant strains. This promising approach leads to an easy procedure for the bulk and rapid production of silver nanoparticles with the added advantage of less time consumption, ecofriendly and cost effective. Based on its potential candidature as antimicrobials, antibiofilm and cytotoxic agents have been convinced armor against ESKAPE pathogens. The AgNPs might be an alternative paradigm of existing antibiotics as a nanoantibiotic in medicinal application. Further additions are the fabrication and cytotoxicity of the AgNPs, both are important tools in this area which are needed to standardize and investigate the toxic measure to neutralize the side effects.

Acknowledgements

This work was supported by the DST Science and Engineering Research Board (SERB), India (Grant number- SERB/LS-267/2014) and Extra Mural Research Funding of Ministry of Ayurveda, Yoga and Naturopathy, Unani, Siddha and Homoeopathy (AYUSH), India [Grant number- Z. 28015/209 /2015-HPC] for providing fellowship and funds to perform this research.

Conflict of interest

Authors have no conflict to report.

References

Abo-State, M.A.M., Partila, A.M., 2015. Microbial production of silver nanoparticles by *Pseudomonas aeruginosa* cell free extract. J. Ecol. Health. Environ. 3, 91–98.
Ali, K., Ahmed, B., Dwivedi, S., Saquib, Q., 2015. Microwave accelerated green synthesis of stable silver nanoparticles with Eucalyptus globulus leaf extract and their antibacterial and antibiofilm activity on clinical isolates. PLoS One. https://doi.org/10.1371/journal.pone.0131178.
Alqadi, M.K., Abonoqtah, O.A., Alzoubi, F.Y., Alzouby, J., Al-jarrah, K., 2014. pH effect on the aggregation of silver nanoparticles synthesized by chemical reduction. Mater. Sci. Pol. 32, 107–111.
Arvizo, R.R., Bhattacharyya, S., Kudgus, R.A., Giri, K., 2012. Intrinsic therapeutic applications of noble metal nanoparticles: past, present and future. Chem. Soci. Rev. 41, 2943–2970.
Balouirin, M., Sadiki, M., Ibnsouda, S.K., 2016. Methods for *in vitro* evaluating antimicrobial activity: a review. J. Pharm. Anal. 6, 71–79.
Bhainsa, K.C., D'Souza, S.F., 2006. Extracellular biosynthesis of silver nanoparticles using the fungus *Aspergillus fumigatus*. Coll. Surf. Biointerfaces 47, 160–164.
Braydich-Stolle, L., Hussain, S., Schlager, J.J., Hofmann, M.C., 2005. *In vitro* cytotoxicity of nanoparticles in mammalian germline stem cells. Toxicol. Sci. 88, 412–419.
Brust, M., Walker, M., Bethell, D., Schiffrin, D.J., 1994. Synthesis of thiol–derivatised gold nanoparticles in a two–phase liquid–liquid system. J. Chem. Soc. Chem. Commun. 7, 801–802.
Buzea, C., Pacheco, I., Robbie, K., 2007. Nanomaterials and nanoparticles: sources and toxicity. Biointerphases 2, MR17–MR71 (ISSN 1559–4106).
Cascio, C., Geiss, O., Franchini, F., Ojea–Jimenez, I., 2015. Detection, quantification and derivation of number size distribution of silver nanoparticles in antimicrobial consumer products. J. Anal. At. Spectrom. 30, 1255–1265.
Chokriwal, A., Madan, M.S., Singh, A., 2014. Biological synthesis of nanoparticles using bacteria and their applications. Am. J. Pharm. Tech. Res. 4, 2249–3387 (ISSN).
Das, V.L., Thomas, R., Varghese, R.T., Soniya, E.V., 2014. Extracellular synthesis of silver nanoparticles by the *Bacillus* strain CS 11 isolated from industrialized area. 3 Biotech 4, 121–126.
Deepak, V., Kalishwaralal, K., Pandian, S.R.K., Gurunathan, S., 2011. Chapter 2: an insight into the bacterial biogenesis of silver nanoparticles, industrial production and scale–up. In: Rai, M., Duran, N. (Eds.), Metal Nanoparticles in Microbiology, https://doi.org/10.1007/978-3-642-18312-6-2.
El–Deeb, B., Mostafa, N.Y., Altalhi, A., Gherbawy, Y., 2013. Extracellular Biosynthesis of silver nanoparticles by bacteria *Alcaligenes faecalis* with highly efficient anti-–microbial property. Int. J. Chem. Eng. 30, 1137–1144.
Erjaee, H., Rajaian, H., Nazifi, S., 2017. Synthesis and characterization of novel silver nanoparticles using *Chamaemelum nobile* extract for antibacterial application. Adv. Nat. Sci. Nanosci. Nanotechnol. 8, 025004. https://doi.org/10.1088/2043-6254/aa690b.
Flemming, H.C., Wingender, J., 2010. The biofilm matrix. Nat. Rev. Microbiol. 8, 623–633.
Franci, G., Falanga, A., Galdiero, S., 2015. Silver nanoparticles as potential antibacterial agents. Molecule 20, 8856–8874.
Heydari, R., Rashidipour, M., 2015. Green synthesis of silver nanoparticles using extract of oak fruit hull (Jaft): synthesis and in vitro cytotoxic effect on MCF–7 cells. Int. J. Breast Cancer. https://doi.org/10.1155/2015/846743. (Article ID 846743).
Holt, J.G., Krieg, N.R., Sneath, P.H.A., Staley, J.T., 1994. Bergy's Manual of Determinative Bacteriology, 9th ed. Williams and Wilkins, Baltimore, USA.
Hong, S., Chen, T., Zhu, Y., Li, A., 2014. Live–cell stimulated raman scattering imaging of alkyne-tagged biomolecules. Angew. Chem. Int. Ed. 53, 5827–5831.
Iravani, S., 2014. Bacteria in nanoparticle synthesis: current status and future prospects. Inter. Scho. Res. Not. 18. https://doi.org/10.1155/2014/359316. (Article ID 359316).
Jha, A.K., Prasad, K., 2010. Biosynthesis of metal and oxide nanoparticles using *Lactobacilli* from yoghurt and probiotic spore tablets. Biotechnol. J. 5, 285–291.
Kannan, R.R.R., Arumugam, R., Ramya, D., Manivannan, K., Anantharaman, P., 2013. Green synthesis of silver nanoparticles using marine macroalga *Chaetomorpha linum*. Appl. Nanosci. 3, 229–233.
Kopp, M., Kollenda, S., Epple, M., 2017. Nanoparticle–Protein Interactions: Therapeutic Approaches and Supramolecular Chemistry. Acc. Chem. Res. 50, 1383–1390. https://doi.org/10.1021/acs.accounts.7b00051.
Kulkarni, R.R., Shaiwale, N.S., Deobagkar, D.N., Deobagkar, D.D., 2015. Synthesis and extracellular accumulation of silver nanoparticles by employing radiation–resistant

Deinococcus radiodurans, their characterization, and determination of bioactivity. Int. J. Nanomed. 10, 963–974.
Kumar, A.S., Abyaneh, M.K., Gosavi, S.W., Kulkarni, S.K., 2007. Nitrate reductase–mediated synthesis of silver nanoparticles from $AgNO_3$. Biotechnol. Lett. 29, 439–445.
Kumar, S., Stecher, G., Tamura, K., 2016. MEGA7: molecular evolutionary genetics analysis version 7.0 for bigger datasets. Mol. Biol. Evol. 33, 1870–1874.
Kushwaha, A., Singh, V.K., Bhartariya, J., Singh, P., 2015. Isolation and identification of *E. coli* bacteria for the synthesis of silver nanoparticles: characterization of the particles and study of antibacterial activity. Eur. J. Exp. Biol. 5, 65–70.
Lindquist, B.A., Furse, K.E., Corcelli, S.A., 2009. Nitrile groups as vibrational probes of biomolecular structure and dynamics: an overview. Phys. Chem. 11, 8119–8132.
Makarov, V.V., Love, A.J., Sinitsyna, O.V., Makarova, S.S., 2014. "Green" nanotechnologies: synthesis of metal nanoparticles using plants. Acta Nat. 6, 35–44.
Markowska, K., Grudniak, A.M., Wolska, K.I., 2013. Silver nanoparticles as an alternative strategy against bacterial biofilms. Acta Biochem. Pol. 60, 523–530.
Matthews, L., Kanwar, R.K., Zhou, S., Punj, V., 2010. Applications of nanomedicine in antibacterial medical therapeutics and diagnostics. Open Trop. Med. J. 3, 1–9.
Medina, R.I., Bashir, S.S., Luo, Z.P., Liu, J.L., 2009. Green synthesis and characterization of polymer–stabilized silver nanoparticles. Coll. Surf. B 73, 185–191.
Meng, Y., 2015. A sustainable approach to fabricating Ag nanoparticles/PVA hybrid nanofiber and its catalytic activity. Nanomaterials 5, 1124–1135.
Ojha, S., Sett, A., Bora, U., 2017. Green synthesis of silver nanoparticles by *Ricinus communis* var. *Carmencita* leaf extract and its antibacterial study. Adv. Nat. Sci. Nanosci. Nanotechnol. 8 (035009), 8. https://doi.org/10.1088/2043-6254/aa724b.
Oladipo, I.C., Lateef, A., Musibau, A.A., Tesleem, B., 2017. Green synthesis and antimicrobial activities of silver nanoparticles using cell free–extracts of *Enterococcus* species. Not. Sci. Biol. 9, 196–203.
Paredes, D., Ortiz, C., Torres, R., 2014. Synthesis, characterization, and evaluation of antibacterial effect of Ag nanoparticles against *Escherichia coli* O157:H7 and methicillin-resistant *Staphylococcus aureus* (MRSA)". Int. J. Nanomed. 9, 1717–1729.
Patil, U.S., Qu, H., Caruntu, D., O'Connor, C.J., 2013. Labeling primary amine groups in peptides and proteins with N–hydroxysuccinimidyl ester modified Fe_3O_4@SiO_2 nanoparticles containing cleavable disulfide–bond linkers. Biol. Chem. 24, 1562–1569.
Patterson, A.L., 1939. The Scherrer formula for X–ray particle size determination. Phys. Rev. 56, 978. https://doi.org/10.1103/PhysRev.56.978.
Qu, F., Xu, H., Wei, H., Lai, W., 2010. Effects of pH and temperature on antibacterial activity of silver nanoparticles. In: Proceedings of the 3rd International Conference on Biomedical Engineering and Informatics. BMEI 2010; 978–1–4244–6498–2.
Ramalingam, K., Amaechi, B.T., Rawls, H.R., Lee, V.A., 2011. Antimicrobial activity of nanoemulsion on cariogenic *Streptococcus mutans*. Arch. Oral Biol. 56, 437–445.
Roy, R., Tiwari, M., Donelli, G., Tiwari, V., 2018. Strategies for combating bacterial biofilms: a focus on anti–biofilm agents and their mechanisms of action. Virulence 9, 522–554.
Rudramurthy, G.R., Swamy, M.K., Sinniah, U.R., Ghasemzadeh, A., 2016. Nanoparticles: alternatives against drug–resistant pathogenic microbes. Molecules 21 (7), 836.
Sambrook, J., 1989. Molecular Cloning: A Laboratory Manual, 2nd ed. Cold spring harbor Laboratory press, Plainview, New York.
Schmieder, R., Edwards, R., 2012. Insights into antibiotic resistance through metagenomic approaches. Future Microbiol. 7, 73–89.
Shahverdi, A.R., Fakhimi, A., Shahverdi, H.R., Minaian, S., 2007a. Synthesis and effect of silver nanoparticles on the antibacterial activity of different antibiotics against *Staphylococcus aureus* and *Escherichia coli*. Nanomed. Nanotechnol. Biol. Med. 3, 168–171.
Shahverdi, A.R., Minaeian, S., Shahverdi, H.R., Jamalifar, H., 2007b. Rapid synthesis of silver nanoparticles using culture supernatants of Enterobacteria: a novel biological approach. Pro. Biochem. 42, 919–923.
Singh, B.R., Dwivedi, S., Al–Khedhairy, A.A., Musarrat, J., 2011. Synthesis of stable cadmium sulfide nanoparticles using surfactin produced by *Bacillus amyloliquifaciens* strain KSU–109. Coll. Surf. B Biointerfaces 85, 207–213.
Singh, P., Kim, Y.J., Wang, C., Mathiyalagan, R., 2016. The development of a green approach for the biosynthesis of silver and gold nanoparticles by using *Panax ginseng* root extract, and their biological applications. Artif. Cells Nanomed. Biotechnol. 44 (4), 1150–1157. https://doi.org/10.3109/21691401.2015.1011809. (ISSN: 2169–1401).
Singh, R., Wagh, P., Wadhwani, S., Gaidhani, S., Kumbhar, A., Bellare, J., Chopade, B.A., 2013. Synthesis, optimization, and characterization of silver nanoparticles from Acinetobacter calcoaceticus and their enhanced antibacterial activity when combined with antibiotics. Int. J. Nanomed. 8, 4277–4290.
Singh, S., Singh, B.R., Khan, W., Naqvi, A.H., 2014. Synthesis and characterization of carbon nanotubes/titaniummolybdate nanocomposite and assessment of its photocatalytic activity. J. Mol. Struct. 1056–1057, 194–201.
Sneath, P.H.A., Sokal, R.R., 1973. Numerical Taxonomy: The Principles and Practice of Numerical Classification. Freeman, San Francisco, pp. 573.
Staszek, M., Siegel, J., Rimpelova, S., Lyutakov, O., Svorcik, V., 2015. Cytotoxicity of noble metal nanoparticles sputtered into glycerol. Mater. Lett. 158, 351–354.
Tiwari, M., Raghav, R., Tiwari, V., 2015. Comparative anti–bacterial activity of differently capped silver nanomaterial on the carbapenem sensitive and resistant strains of *Acinetobacter baumannii*. J. Nanomed. Nanotechnol. 6, 314. https://doi.org/10.4172/2157-7439.1000314.
Vanaja, M., Annadurai, G., 2013. *Coleus aromaticus* leaf extract mediated synthesis of silver nanoparticles and its bactericidal activity. Appl. Nanosci. 3, 217–223.
Verma, S.K., Jha, E., Panda, P.K., Mishra, A., 2018. Rapid novel facile biosynthesized silver nanoparticles from bacterial release induce biogenicity and concentration dependent in vivo cytotoxicity with embryonic zebrafish-A mechanistic insight. Toxicol. Sci. 16, 12–138.
Vogt, C., Pernemalm, M., Kohonen, P., Laurent, S., Hultenby, K., Vahter, M., Lehtio, J., Toprak, M.S., Fadeel, B., 2015. Proteomics analysis reveals distinct corona composition on magnetic nanoparticles with different surface coatings: implications for interactions with primary human macrophages. PLoS One 2015 (10), e0129008.
Wei, D., Qian, W., 2008. Facile synthesis of Ag and Au nanoparticles utilizing chitosan as a mediator agent. Coll. Surf. B Biointerfaces 62, 136–142.
Weisburg, W.G., Brans, S.M., Pilletier, D.A., Lane, D.J., 1991. 16s ribosomal DNA amplification for phylogenetic study. J. Bacteriol. 173, 697–703.
Winter, J.M., Moore, B.S., 2009. Exploring the chemistry and biology of vanadium-dependent haloperoxidases. J. Biol. Chem. 284, 18577–18581.